

Constraints on Ω_Λ and Ω_m from Distant Type 1a Supernovae and Cosmic Microwave Background Anisotropies

G. Efstathiou¹, S. L. Bridle², A.N. Lasenby², M.P. Hobson², R.S. Ellis¹

¹ Institute of Astronomy, Madingley Road, Cambridge, CB3 0HA.

² Cavendish Astrophysics Group, Cavendish Laboratory, Madingley Road, Cambridge CB3 OHE.

4 December 2017

ABSTRACT

We perform a combined likelihood analysis of the latest cosmic microwave background anisotropy data and distant Type 1a Supernova data of Perlmutter *et al.* (1998a). Our analysis is restricted to cosmological models where structure forms from adiabatic initial fluctuations characterised by a power-law spectrum with negligible tensor component. Marginalizing over other parameters, our best fit solution gives $\Omega_m = 0.25^{+0.18}_{-0.12}$ and $\Omega_\Lambda = 0.63^{+0.17}_{-0.23}$ (95% confidence errors) for the cosmic densities contributed by matter and a cosmological constant respectively. The results therefore strongly favour a nearly spatially flat Universe with a non-zero cosmological constant.

1 INTRODUCTION

The aim of this paper is to constrain the geometry of the Universe by combining results from the cosmic microwave background anisotropies (CMB) with those from distant Type 1a supernovae. Recently, there have been a number of analyses of CMB anisotropies aimed at constraining cosmological parameters (Hancock *et al.* 1998, Bond and Jaffe 1997, Lineweaver and Barbosa 1998a,b, Webster *et al.* 1998). These papers show that the CMB already provides useful constraints on adiabatic inflationary models. The results described in this paper extend these analyses to a wider parameter set including closed Universes.

However, observations of CMB anisotropies alone cannot determine the geometry of the Universe unambiguously (Bond, Efstathiou and Tegmark 1997, Zaldarriaga, Spergel and Seljak 1997). This is because two models with identical fluctuation spectra and matter content will have nearly identical CMB power spectra if they have the same angular diameter distance to the last scattering surface. This *geometrical degeneracy* can be broken for extreme values of the cosmological parameters Ω_Λ and Ω_m by the inhomogeneous Sachs-Wolfe effect at low multipoles (see Efstathiou and Bond 1998), but for plausible parameters the degeneracy is nearly exact. *

A number of authors (White 1998, Tegmark *et al.* 1998, Efstathiou and Bond 1998) have shown that the magnitude-redshift relation for distant Type 1a supernovae (SN) provides nearly orthogonal constraints in the Ω_Λ – Ω_m plane to those derived from the CMB. The combination of CMB and SN data can thus provide tight constraints on the geome-

try of the Universe. This has been demonstrated by White (1998), Garnavich *et al.* (1998) and Lineweaver (1998) using the SN data of Perlmutter *et al.* (1997, 1998b) and Riess *et al.* (1998). In this paper, we use the larger sample of 42 high-redshift SN of Perlmutter *et al.* (1998a, hereafter P98, 1998b). The likelihood analysis of the CMB observations is described in Section 2. Section 3 describes the likelihood analysis of the SN data and the results from the combined data set are described in Sections 4 and 5.

2 ANISOTROPIES OF THE COSMIC MICROWAVE BACKGROUND

The analysis presented here is similar to that described by Hancock *et al.* (1998) and we refer the reader to this paper for technical details. Similar analyses and compilations of observations are discussed by Lineweaver (1998, and references therein) and by Bond, Jaffe and Knox (1998). A window function W_l for each experiment is used to convert the observed level of anisotropy to flat bandpower estimates $(\Delta T_l/T) \pm \sigma$ centred on the effective multipole l_{eff} (defined as the half-power point of the window function). The resulting CMB data points are plotted in Figure 1, together with their 68 per cent confidence limits. These confidence limits have been obtained using likelihood analyses and hence incorporate uncertainties due to random errors, sampling variance and cosmic variance.

The data points in Figure 1 are identical to those given in Webster *et al.* (1998) except that we have added the three QMAP points (Ka and Q bands for flights 1 and 2, Devlin *et al.* 1998, Herbig *et al.* 1998, De Oliveira-Costa *et al.* 1998).

We fit the CMB data points to adiabatic CDM models specified by the following parameters: (1) amplitude Q_{10} of the $\ell = 10$ multipole defined as in Lineweaver (1998); (2) the

* Gravitational lensing of the CMB can break this degeneracy however (see Seljak and Zaldarriaga 1998).

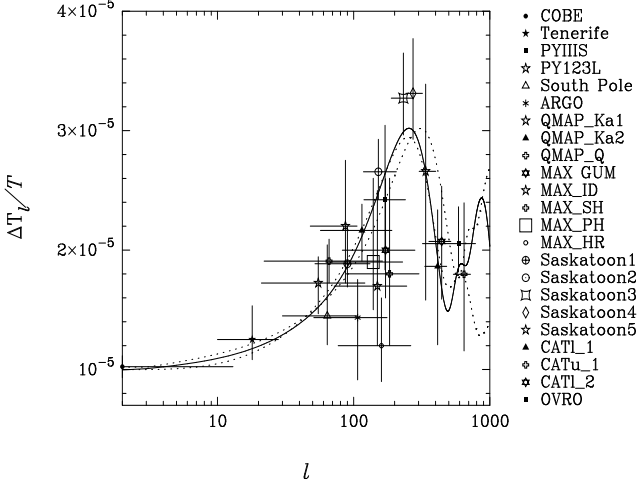


Figure 1. CMB bandpower anisotropy estimates for various experiments, as described in the text. The solid line shows the best fitting adiabatic CDM model with parameters $Q_{10} = 1.14$, $n = 1.08$, $\omega_c = 0.36$, $\omega_b = 0.03$ and Doppler peak location parameter $\gamma_D = 1.18$. The dotted lines show the best fitting curves with location parameter fixed at $\gamma_D = 0.8$ and $\gamma_D = 1.5$ (approximately the 2σ allowed range for γ_D).

density parameters Ω_k and (3) Ω_Λ ; (4) the scalar spectral index n_s ; (5) the physical density in cold dark matter $\omega_c = \Omega_c h^2$ [†]; (6) the physical density in baryons $\omega_b = \Omega_b h^2$. We ignore tensor modes in this analysis.[†]

The motivation for choosing this set of variables is explained in Efstathiou and Bond (1998, hereafter EB98). The physical densities ω_c and ω_b and the radiation density determine the sound speed at the time of recombination. The geometry of the universe is specified by the parameters Ω_k and Ω_Λ , and the Hubble constant enters as an auxiliary parameter

$$h = \left[\frac{(\omega_c + \omega_b)}{(1 - \Omega_k - \Omega_\Lambda)} \right]^{1/2}. \quad (1)$$

We have fitted the observations to the theoretical models using two methods. Firstly, we compute a grid of theoretical power spectra in the parameters Ω_k , Ω_Λ , n_s , ω_c , using the CMBFAST code of Seljak and Zaldarriaga (1996) with ω_b constrained to 0.019, the value inferred from primordial nucleosynthesis and the deuterium abundances measured from quasar spectra ($\omega_b = 0.019 \pm 0.001$, see Burles and Tytler 1998a,b). In its present form, the CMBFAST code is restricted to open and spatially flat models ($\Omega_k \geq 0$) and so we have adopted a second, approximate, technique to extend the theoretical predictions to closed models. This is based on a semi-analytic fitting formula for the CMB power spectrum of $\Omega_k = 0$ models, which is a generalization of the fitting formula of equation (24) in EB98 and provides accu-

[†] Here h is the Hubble constant in units of $100 \text{ km s}^{-1} \text{ Mpc}^{-1}$.

[‡] For reasonable amplitudes of a tensor mode, the effect on the position of the first Doppler peak is small. A small tensor mode will therefore have little effect on the cosmological parameters Ω_Λ and Ω_m since these are determined primarily by the position of the first Doppler peak.

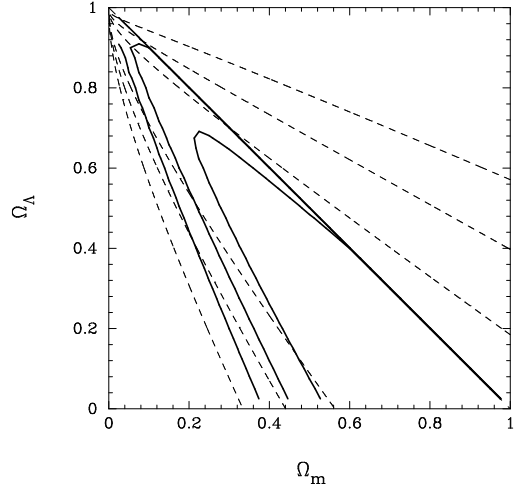


Figure 2. Likelihood contours in the $\Omega_\Lambda - \Omega_m$ plane derived from the CMB data points shown in Figure 1. The contours are plotted where $-2\ln\mathcal{L}/\mathcal{L}_{max}$ is equal to 2.29, 6.16 and 11.83, corresponding approximately to 1, 2 and 3σ confidence contours for a Gaussian likelihood function. The solid lines show the marginalized likelihood contours derived from the CMBFAST computations for $\omega_b = 0.019$. The dotted lines extending into the $\Omega_k < 0$ region show the equivalent contours derived from the fitting function approach described in the text. For the dotted contours, we have marginalized over ω_b , although this has very little effect.

rate fits to the first three Doppler peaks of the CMB power spectrum. The fitting formula includes the dependences on n_s , ω_b , ω_c and Ω_Λ and is typically accurate to better than 5 percent. For models with non-zero values of Ω_k , we use the scaling relation $C(\ell') \rightarrow C(\ell\gamma_D)$, where γ_D is a ‘location’ parameter,

$$\gamma_D \approx \frac{\ell_D(\Omega_k, \Omega_\Lambda)}{\ell_D(\Omega_k = 0, \Omega_\Lambda = 0)}, \quad (2)$$

where $\ell_D(\Omega_k, \Omega_\Lambda)$ is the location of the first Doppler peak given by equation (22) of EB98 generalized to models with $\Omega_k < 0$. The location parameter thus measures the positions of the Doppler peaks relative to those of a spatially flat model with zero cosmological constant. The approximate formula does not include the inhomogeneous Sachs-Wolfe effect (see *e.g.* Bond 1996) which affects low multipoles if Ω_k and Ω_Λ are non-zero. However, the inhomogeneous Sachs-Wolfe effect is a weak discriminator of cosmological models (see EB98) and, with the data shown in Figure 1, the constraints on cosmological models are set primarily by the location of the first Doppler peak. A similar approximate technique, using rescaling of power spectra computed with CMBFAST, is described by Tegmark (1998).

Figure 1 shows the best fitting CMB power spectrum, together with the best fitting curves with $\gamma_D = 0.8$ and 1.5 (spanning the 2σ allowed range of γ_D after marginalization over other parameters). The present CMB data points evidently favour models with $\Omega_k \approx 0$. The large number of data points at $\ell \sim 100$ set quite strong constraints on closed models, but the lack of data points at $\ell \gtrsim 300$ leads to weaker constraints on open models. The CMB data do not yet allow strong constraints on the parameters ω_b and ω_c , hence the constraints on Hubble constant (equation 1) are also extremely weak.

Figure 2 shows the CMB constraints in the $\Omega_m - \Omega_\Lambda$

plane. Here, we have marginalized over n_s , Q_{10} , ω_c (and ω_b for the likelihoods computed from the fitting formula) assuming uniform prior distributions in these parameters. The marginalized likelihood depends slightly on the range adopted for ω_c ; in Figure 2 we assume a uniform prior distribution over the range $0.05 \leq \omega_c \leq 0.5$. The marginalized likelihood function is insensitive to the ranges and priors adopted for the other parameters and is insensitive to ω_b .

The results of this analysis are similar to those of Lineweaver (1998) and Tegmark (1998) but differ in detail. The main difference is in the way that we marginalize over the likelihood function. We have assumed a uniform prior distribution in each parameter and performed direct integrations over the full likelihood function. Lineweaver and Tegmark ‘marginalize’ over a subset of parameters by fixing them to their maximum likelihood values. Our approach provides more robust errors, though the marginalized likelihood function for poorly determined parameters will depend on the choice of prior (usually weakly). In the limit that the likelihood function is Gaussian, the two approaches are equivalent. However, for non-Gaussian likelihoods (as is the case with the present CMB data) the approach adopted by Lineweaver and Tegmark can give misleadingly small errors on some parameters.

3 MAGNITUDE-REDSHIFT RELATION FOR DISTANT SUPERNOVAE

We use the sample of 42 high redshift ($0.18 \leq z \leq 0.83$) supernovae of P98, supplemented with 18 low redshift ($z < 0.1$) Type 1a supernovae from the Calán/Tololo Supernova Survey (Hamuy *et al.* 1996). For each supernova, P98 computed a peak magnitude in the B band m_B , corrected for Galactic extinction and a ‘stretch parameter’ s that stretches the time axis of a template Type 1a lightcurve to match the observed lightcurve (see Perlmutter *et al.* 1995, 1997).

P98 provide a comprehensive analysis of the constraints on Ω_m and Ω_Λ derived from the SN magnitude-redshift relation and of the effects of excluding various outlying SN, including or excluding corrections for the lightcurve width-luminosity relation, host galaxy extinction, *etc.* P98 show that the likelihood function in the Ω_m – Ω_Λ plane is remarkably stable to such changes. We do not repeat this analysis here, but instead concentrate on the analysis of the supernovae used in the ‘primary fit’ of P98 (their fit C) which excludes 4 high redshift objects. These are, SN 1997O, 1996cg and 1996cn, which are very likely reddened by their host galaxies and so are fainter than the best fitting magnitude redshift relation, and SN 1994H which is not spectroscopically confirmed as a Type 1a SN and lies brighter than the best-fit relation. In agreement with the results of P98, none of our conclusions change significantly if we include these supernovae.

We define a corrected peak magnitude m_B^{corr} for the lightcurve width-luminosity effect

$$m_B^{\text{corr}} = m_B + \alpha(s - 1), \quad (3)$$

where s is the measured stretch factor and α is a constant to be determined. These corrected magnitudes are compared to the predicted magnitudes

Table 1: Maximum Likelihood Parameters

\mathcal{M}_B	α	Ω_m	Ω_Λ	sample
-3.45	1.33	0.54	1.09	combined
-3.69	1.41	0.75	1.86	high z
-3.37	1.32	–	–	low z

$$m_B^{\text{pred}}(z) = \mathcal{M}_B + 5\log\mathcal{D}_L(z, \Omega_m, \Omega_\Lambda), \quad (4)$$

where \mathcal{M}_B is related to the corrected absolute magnitude M_B by $\mathcal{M}_B = M_B - 5\log H_0 + 25$, and $\mathcal{D}_L = d_L + 5\log H_0$ is the Hubble-constant-free luminosity distance defined by P98. To compute the luminosity distance, we ignore gravitational lensing and use the standard expression for a Universe with uniform density (see *e.g.* Peebles 1993),

$$d_L(z, \Omega_m, \Omega_\Lambda) = \frac{c}{H_0} \frac{(1+z)}{|\Omega_k|^{1/2}} \sin_k [|\Omega_k|^{1/2} x(z, \Omega_m, \Omega_\Lambda)],$$

$$x(z, \Omega_m, \Omega_\Lambda) = \int_0^z \frac{dz'}{[\Omega_m(1+z')^3 + \Omega_k(1+z')^2 + \Omega_\Lambda]^{1/2}} \quad (5)$$

where $\Omega_k = 1 - \Omega_m - \Omega_\Lambda$ and $\sin_k = \sinh$ if $\Omega_k > 0$ and $\sin_k = \sin$ for $\Omega_k < 0$. We assume a constant cosmological constant here rather than an arbitrary equation of state as might arise with scalar fields that become important at late times (Ratra and Peebles 1988, Caldwell, Dave and Steinhardt 1998). The biases in the magnitude-redshift relation arising from gravitational lensing should be negligible for CDM-like models unless a large fraction of the dark matter is in compact objects (*e.g.* Wambsganss, Cen and Ostriker 1998). Even in the latter case, P98 show that the biases are relatively small for the low matter densities favoured by the SN data.

With the above assumptions, we perform a four parameter (Ω_m , Ω_Λ , \mathcal{M}_B and α) likelihood analysis assuming Gaussian errors on m_B^{corr} consisting of three terms,

$$(\Delta m_B^{\text{corr}})^2 = \Delta m_B^2 + \alpha^2 \Delta s^2 + \Delta m_{\text{intrinsic}}^2, \quad (6)$$

where Δm_B and Δs are the measurement errors in m_B and s and $\Delta m_{\text{intrinsic}}$ is the intrinsic dispersion in m_B determined to be 0.18 mag from the Calán/Tololo sample. (The maximum likelihood parameters are extremely insensitive to $\Delta m_{\text{intrinsic}}$.) This analysis differs from that in P98 in that we include the dependence of the magnitude errors on the parameter α self-consistently in the likelihood analysis via equation (6). As we will see below this has little effect on the likelihood constraints on Ω_Λ and Ω_m (Figure 3), which are in good agreement with the results presented in P98. However, our analysis allows an important test of the intrinsic properties of high and low redshift supernovae (see Figure 4).

Excluding the four SN as described above, we analyse the combined high redshift P98 + Calán/Tololo samples (denoted ‘combined’), and the two samples separately (denoted ‘high z’ and ‘low z’ respectively). The magnitude-redshift relation of the low z sample is relatively insensitive to cosmology, hence we fix $\Omega_m = 1$ and $\Omega_\Lambda = 0$ in the likelihood analysis. Table 1 lists the parameters that maximize the likelihood for these samples.

Figure 3 shows the likelihood function for the combined sample in the Ω_m – Ω_Λ plane after marginalization over the parameters \mathcal{M}_B and α assuming uniform prior distributions

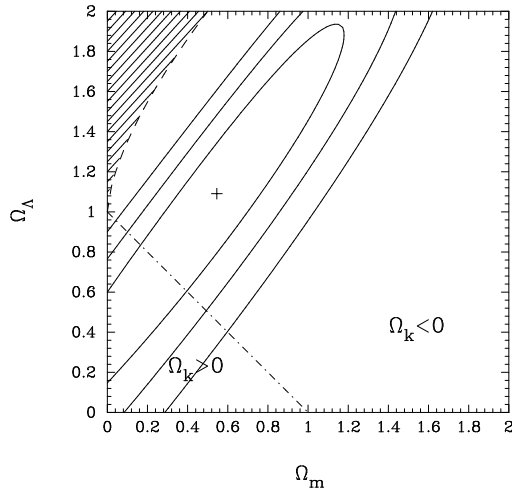


Figure 3. Likelihood contours (1, 2 and 3σ , as defined in the caption to Figure 2) in the Ω_Λ – Ω_m plane derived from the SN magnitude-redshift relation after marginalization over the parameters \mathcal{M}_B and α . The cross shows the maximum likelihood solution. Bouncing universes have parameters within the hatched region.

in these variables. We use this likelihood function in Section 3 when we combine the SN sample with parameters derived from the CMB. As P98 show (and we have confirmed) changes in the analysis, *e.g.* omitting outliers, stretch correction, reddened objects, usually shifts the error ellipses by much less than the width of the 1σ contour.

An important consistency check is the agreement between the intrinsic properties of the high and low redshift SN. This is illustrated in Figure 4 which shows likelihood contours for the parameters \mathcal{M}_B and α for the low z and high z samples (marginalized over Ω_Λ and Ω_m for the high z sample). This diagram shows that the low z and high z samples have the same lightcurve width-luminosity relation and consistent peak absolute magnitudes \mathcal{M}_B . (Note, however, that the contours for the high z sample become highly elongated in the \mathcal{M}_B direction because this parameter correlates strongly with Ω_Λ and Ω_m). We have repeated the likelihood analysis including the intrinsic magnitude scatter $\Delta m_{\text{intrinsic}}$ as a free parameter. For the low- z sample, the likelihood gives a broad distribution peaked at $\Delta m_{\text{intrinsic}} = 0.18$, consistent with the *rms* residual of 0.16 magnitude of the Calán/Tololo points around the best fit solution. The combined sample gives $\Delta m_{\text{intrinsic}} = 0.20$, slightly higher but consistent with the low- z sample. (In fact, $\Delta m_{\text{intrinsic}}$ drops to 0.18 mag if we remove three outliers, SN92bi, SN95as and SN97K).

For low redshift supernovae, the lightcurve widths and luminosities are known to correlate with the morphological type of the host galaxies (Hamuy *et al.* 1996). Thus the lack of any significant difference between the high and low redshift samples in Figure 2 provides a constraint on evolutionary corrections associated with systematic changes in the host galaxies with redshift (*e.g.* metallicity, morphological mix). Figure 4 therefore indicates no detectable evolutionary trends in the underlying supernova population used in this analysis.

Table 1 shows that the high z sample alone yields val-

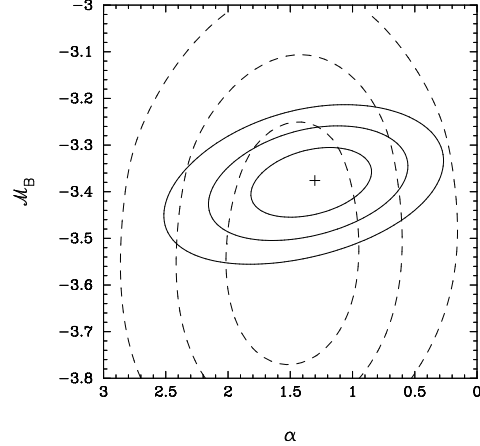


Figure 4. Likelihood contours (1, 2 and 3σ) in the \mathcal{M}_B – α plane. The solid lines show contours for the Calán/Tololo sample and the dotted lines show contours for the high redshift P98 sample after marginalization over the cosmological parameters Ω_Λ and Ω_m .

ues for Ω_m and Ω_Λ that are similar to those of the combined sample. However, the error contours for the high z sample are much larger than those shown in Figure 1 for the combined sample so that an $\Omega_m = 1$, $\Omega_\Lambda = 0$ universe lies within the 2σ contour. The narrowness of the likelihood contours shown in Figure 3 therefore rely on combining the P98 data with the Calán/Tololo sample, though the general trends are evident in the high- z sample alone.

In summary, the P98 and Calán/Tololo SN strongly favour a universe with $0.78\Omega_m - 0.62\Omega_\Lambda \approx -0.25 \pm 0.13$. This is consistent with the analysis of P98 (who find $0.8\Omega_m - 0.6\Omega_\Lambda \approx -0.2 \pm 0.1$) and with the analysis of a sample of 16 SN at $z > 0.16$ (14 of which are independent of the P98 high redshift sample) combined with 34 low z SN from the Calán/Tololo and CfA samples (Riess *et al.* 1998, Garnavich *et al.* 1998). Furthermore, the lightcurve width-luminosity relation of the high z SN is consistent with that of the nearby sample suggesting that these objects have similar intrinsic properties. If an evolutionary effect is causing a systematic error in the magnitude-redshift relation of the distant sample, then it must be so as to preserve the lightcurve width-luminosity relation.

4 COMBINING THE SUPERNOVAE AND CMB LIKELIHOODS

4.1 Combined likelihoods

The combined likelihood obtained by multiplying the SN and CMB likelihoods are shown in Figure 5. As in Figure 2, the solid lines show the likelihood computed with CMB-FAST and the dashed lines show the approximate technique indicating how the contours extend into the $\Omega_k < 0$ regime. The likelihood peaks at $\Omega_m = 0.25$ and $\Omega_\Lambda = 0.63$. The combined likelihood thus strongly favours a nearly spatially flat Universe with a low matter density and high cosmological constant. In fact, the 2σ ellipse in Figure 5 extends over the range $\Omega_m \approx 0.12$, $\Omega_\Lambda = 0.84$, to $\Omega_m \approx 0.49$ and $\Omega_\Lambda = 0.51$. A high value of Ω_Λ is suggested by the SN data alone, and is required if we impose the constraint $\Omega_k = 0$ (see Figure 7 of P98; Figure 6 Riess *et al.* 1998). However, from the SN data

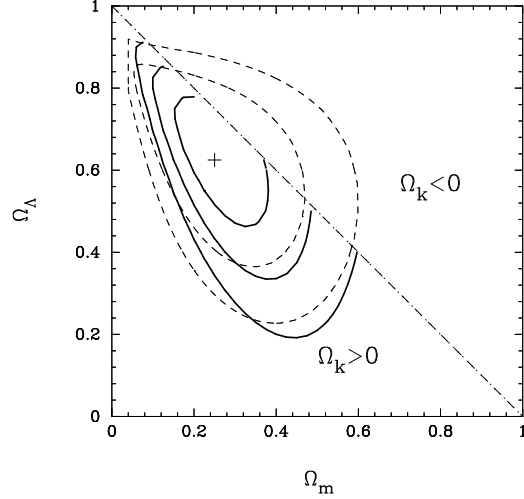


Figure 5. Likelihood contours derived by combining the supernovae likelihood function shown in Figure 3 with the CMB likelihood function shown in Figure 2. As in Figure 2, solid contours show 1, 2 and 3 σ confidence intervals computed using CMBFAST. The dashed contours show 2 and 3 σ contours computed using the approximate CMB fitting technique (for clarity we do not plot the 1 σ contour). The combined CMB+SN likelihood function peaks at $\Omega_m = 0.25$ and $\Omega_\Lambda = 0.63$

alone we cannot rule out an open Universe with a low matter density $\Omega_m \lesssim 0.1$ and zero cosmological constant. Since the CMB data favour a universe with $\Omega_k = 0$, the combined SN+CMB data *require a non-zero cosmological constant at a high significance level*. This is the main result of this paper.

Figure 6 provides another illustration of how the combination of CMB and SN data dramatically improve the constraints on Ω_Λ and Ω_m . Here we have plotted the likelihood functions marginalized over all other parameters except Ω_m (Figure 6a) and Ω_Λ (Figure 6b) for the SN and CMB data alone and for the combined data sets. For a Gaussian likelihood function, the 95% confidence region is delineated by $\mathcal{L}/\mathcal{L}_{\max} \geq 0.146$ and so we can see from Figure 6 that the constraints on Ω_m and Ω_Λ from the SN and CMB data alone are extremely weak. However, for the combined data sets we find $\Omega_m = 0.25^{+0.18}_{-0.12}$ and $\Omega_\Lambda = 0.63^{+0.17}_{-0.23}$ at the 95% confidence level.

4.2 Systematic errors

Systematic errors in the analysis of the SN data are discussed at length by P98 and by Riess *et al.* 1998. No systematic error has yet been identified that could produce a large downward shift of the SN likelihood contours in Figure 3. Possible sources of systematic error include differences in the reddening caused by the host galaxies, and evolutionary (*e.g.* metallicity dependent) corrections to the SN absolute magnitude-redshift relation. Internal reddening for this sample is discussed in detail by P98. They find no excess reddening of most of the distant SN when compared to the Calán/Tololo sample, although there are a small number of possibly reddened SN (three of which have been excluded in this analysis). The inclusion or exclusion of these reddened objects does not significantly affect Figure 5. Grey extinction is much harder to rule out, but may not be physically well motivated.

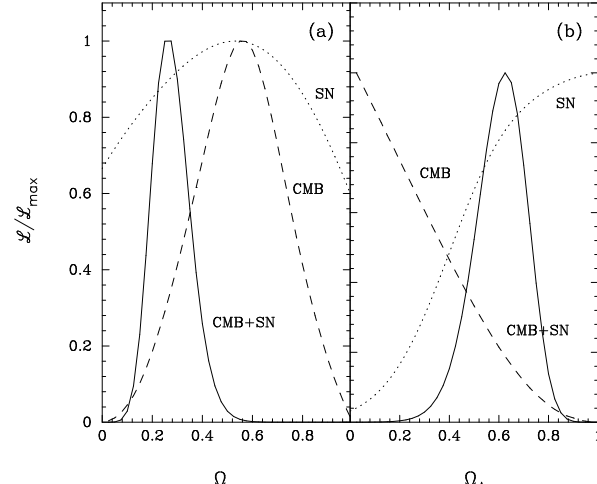


Figure 6. Marginalized likelihood functions plotted as function of Ω_m (left hand panel) and Ω_Λ (right hand panel). The dotted lines are for the SN data alone (Figure 3), dashed lines for the CMB data alone (Figure 2) and solid lines for the combined data sets (Figure 5).

Possible evolutionary effects are difficult to check. However, the results summarized in Figure 4 show that the high and low redshift SN sample have statistically indistinguishable internal properties, *i.e.* they have consistent lightcurve width-luminosity relations and (within rather large errors) consistent peak absolute magnitudes \mathcal{M}_B . With a larger sample of SN it should be possible to refine this test and to test for differences in the distribution of lightcurve shapes with redshift. Another consistency check would be provided by extending the SN sample to $z > 1$. As Goobar and Perlmutter (1995) have discussed, the degeneracy of the magnitude-redshift relation in the $\Omega_m - \Omega_\Lambda$ plane can be broken by a sample of SN spanning a sufficiently wide range of redshifts.

4.3 The best fit Universe

If systematic errors are indeed small, the combined CMB and SN data strongly favour a near-spatially flat Universe with $\Omega_m \approx 0.25$ and $\Omega_\Lambda \approx 0.63$. These values are close to those favoured by a number of other arguments, which we summarize briefly below (see also *e.g.* Ostriker and Steinhardt 1995, P98, and references therein).

Age & Hubble constant: For our best fit cosmology, the age of the Universe is $14.6(h/0.65)^{-1}$ Gyr (in agreement with P97). This is compatible with recent estimates of 11.5 ± 1.3 Gyr for the ages of the oldest globular clusters (see Chaboyer 1998) and with recent values of H_0 derived from Type 1a supernovae and Cepheid distances, which fall within the range $H_0 = 65 \pm 10 \text{ km s}^{-1} \text{Mpc}^{-1}$ (*e.g.* Freedman *et al.* 1998).

Large-scale structure: Observations of large-scale structure (see *e.g.* Efstathiou 1996 for a review) are consistent with scale-invariant adiabatic cold dark matter universes if $\Gamma \approx \Omega_m h \approx 0.2-0.3$. This is broadly consistent with the analysis presented here and with the analysis of combined CMB and IRAS galaxy data presented by Webster *et al.* (1998).

Baryon abundance in clusters: Consistency between primordial nucleosynthesis ($\omega_b \approx 0.019$) and the ratio of baryons in clusters to total cluster mass ($f_b \approx 0.06h^{-3/2}$, see Evrard

1998 and references therein) requires a low matter density, $\Omega_m \approx 0.26(h/0.65)^{-1/2}$, consistent with the best fit solution of Figure 5.

5 CONCLUSIONS

- We have applied an approximate formula for the CMB power spectrum that can be used to constrain a wide set of cosmological parameters, including closed universes, by fitting to the CMB anisotropy data. The results agree well with those derived from exact computations using the CMB-FAST code.
- In our analysis we perform a proper marginalization over parameters, assuming uniform prior distributions, to derive constraints in the Ω_m - Ω_Λ plane and on Ω_m and Ω_Λ separately.
- Current CMB anisotropy data provide strong constraints on the position of the first Doppler peak and favour a spatially flat Universe.
- A likelihood analysis of the SN data provides robust constraints on Ω_m and Ω_Λ consistent with those derived by P98. For a spatially flat Universe, the SN data require a non-zero cosmological constant at a high level of significance ($\Omega_\Lambda \gtrsim 0.5$ at 95 % confidence).
- The lightcurve width-luminosity relation for high redshift and low redshift SN are statistically indistinguishable, consistent with no evolution of the SN population.
- The combination of CMB and SN data thus provide strong constraints on Ω_m and Ω_Λ favouring values of $\Omega_m \approx 0.25$ and $\Omega_\Lambda \approx 0.63$. If there are no significant systematic effects in the SN data (e.g. grey dust, evolution) then we are forced into accepting a cosmological constant or a “quintessence”-like component of the Universe (Caldwell *et al.* 1998, Garnavich *et al.* 1998).
- There are a number of independent lines of argument, *e.g.* the age of the Universe, large-scale clustering of galaxies and the baryon content of clusters, to support the best-fit parameters derived in this paper.

Acknowledgements. G. Efstathiou thanks PPARC for the award of a Senior Fellowship. S. Bridle acknowledges the receipt of a PPARC studentship. We thank the members of the Supernova Cosmology Project for allowing us to use their data, especially Saul Perlmutter, who provided many helpful comments on this manuscript, and also Mike Irwin and Gerson Goldhaber for discussions of the P98 analysis.

REFERENCES

Bond, J.R. 1996, *Theory and Observations of the Cosmic Background Radiation*, in “Cosmology and Large Scale Structure”, Les Houches Session LX, August 1993, eds. R. Schaeffer, J. Silk, M. Spiro and J. Zinn-Justin, Elsevier Science Press, Amsterdam, p469.

Bond J.R., Efstathiou G., Tegmark M., 1997, MNRAS, 291 L33.

Bond, J.R., Jaffe, A. 1997, in Proc. XXXI Rencontre de Moriond, ed. F. Bouchet, Edition Frontières, in press; astro-ph/9610091.

Bond J.R., Jaffe A.H. and Knox L.E., 1998. astro-ph/9808264.

Burles S., Tytler D., 1998a, to appear in the Proceedings of the Second Oak Ridge Symposium on Atomic & Nuclear Astrophysics, ed. A. Mezzacappa, Institute of Physics, Bristol. astro-ph/9803071

Burles S., Tytler D., 1998b, ApJ, in press. astro-ph/9712109

Caldwell, R.R., Dave, R., Steinhardt P.J., 1998, Phys Rev Lett, 80, 1582.

Carroll S.M., Press W.H., Turner E.L., 1992, Ann. Rev. Astr. Astrophys., 30, 499.

Chaboyer B., 1998, astro-ph/9808200.

Devlin M.J., De Oliveira-Costa A., Herbig T., Miller A.D., Netterfield C.B., Page L., Tegmark M., 1998, submitted to ApJL. astro-ph/9808043.

Efstathiou G. 1996, *Observations of Large-Scale Structure in the Universe*, in “Cosmology and Large Scale Structure”, Les Houches Session LX, August 1993, eds. R. Schaeffer, J. Silk, M. Spiro and J. Zinn-Justin, Elsevier Science Press, Amsterdam, p135.

Efstathiou G., Bond J.R., MNRAS in press. astro-ph/9807130.

Evrard G., 1998, submitted to MNRAS. astro-ph/9701148.

Freedman J.B., Mould J.R., Kennicutt R.C., Madore B.F., 1998, astro-ph/9801090.

Garnavich P.M. *et al.* 1998, astro-ph/9806396.

Goobar A., Perlmutter S., 1995, ApJ, 450, 14.

Hamuy M., Phillips M.M., Maza J., Suntzeff N.B., Schommer R.A., Aviles R. 1996, AJ, 112, 2391.

Hancock S., Gutierrez C.M., Davies R.D., Lasenby A.N., Rocha G., Rebolo R., Watson R.A., Tegmark M., 1997, MNRAS, 298, 505

Hancock S., Rocha G., Lasenby A.N., Gutierrez C.M., 1998, MNRAS, 294, L1

Herbig T., De Oliveira-Costa A., Devlin M.J., Miller A.D., Page L., Tegmark M., 1998, submitted to ApJL. astro-ph/9808044.

Lineweaver C.H., 1998. ApJ, 505, L69.

Lineweaver, C.H., Barbosa D., 1998a, ApJ, 446, 624.

Lineweaver, C.H., Barbosa D., 1998b, A&A, 329, 799.

De Oliveira-Costa A., Devlin M.J., Herbig T., Miller A.D., Netterfield C.B. Page L., Tegmark M., 1998, submitted to ApJL. astro-ph/9808045.

Ostriker J.P., Steinhardt P.J., 1995, Nature, 377, 600.

Peebles P.J.E., 1993, *Principles of Physical Cosmology*, Princeton University Press, Princeton, New Jersey.

Perlmutter S. *et al.*, 1995, In Presentations at the NATO ASI in Aiguablava, Spain, LBL-38400; also published in Thermonuclear Supernova, P. Ruiz-Lapuente, R. Cana and J. Isern (eds), Dordrecht, Kluwer, 1997, p749.

Perlmutter S. *et al.*, 1997, ApJ, 483, 565.

Perlmutter S. *et al.*, 1998a, ApJ, in press. (P98). astro-ph/9812133.

Perlmutter S. *et al.*, 1998b, In Presentation at the January 1998 Meeting of the American Astronomical Society, Washington D.C., LBL-42230, available at www-supernova.lbl.gov; B.A.A.S., volume 29, p1351, 1997.

Perlmutter S. *et al.*, 1998c, Nature, 391, 51.

Ratra B., Peebles P.J.E., 1988, Phys Rev D 37, 3406.

Riess A. *et al.* 1998, AJ, in press. astro-ph/9805201.

Seljak U., Zaldarriaga M. 1996, ApJ, 469, 437.

Seljak U. & Zaldarriaga M., 1998, astro-ph/9811123.

Tegmark M., 1997, Phys Rev. Lett, 79, 3806.

Tegmark M. 1998, submitted to ApJL. astro-ph/9809201.

Tegmark, M., Eisenstein D.J., Hu W., Kron R.G., 1998, astro-ph/9805117.

Wambsganss J., Cen R., Ostriker J.P., 1998, ApJ, 494, 29.

Webster M., Bridle S.L., Hobson M.P., Lasenby A.N., Lahav O., Rocha, G., 1998, ApJL, in press, astro-ph/9802109.

White M., 1998, ApJ in press. astro-ph/9802295.

Zaldarriaga, M., Spergel D.N., Seljak U., 1997 ApJ, 488, 1.